JOURNAL OF CATALYSIS 100, 196–209 (1986)

Structure and Chemisorptive Properties of the Pt_3Ti Surface

U. BARDI

Dipartimento di Chimica, Universita di Firenze, 50121 Florence, Italy

AND

D. DAHLGREN[1] AND P. N. ROSS

Materials and Molecular Research Division, Lawrence Berkeley Laboratory, Berkeley, California 94720

Received September 4, 1985; revised February 25, 1986

Low-energy electron diffraction (LEED), X-ray photoelectron spectroscopy (XPS), and Auger electron spectroscopy (AES) were used to determine the structure and composition of the surfaces of [111] and [100] oriented crystals of an ordered alloy of bulk stoichiometry Pt_3Ti. Thermal desorption spectroscopy (TDS) was used to study the adsorption of carbon monoxide and hydrogen on these surfaces. The clean, annealed surface of [111] orientation has the ordered structure expected from truncation of the bulk crystal, consisting of alternating atom rows of (50% Pt + 50% Ti) and 100% Pt. The surface of [100] orientation also has a regular truncation structure with the outermost layer being 50% Ti in a $c(2 \times 2)$ lattice and the second layer, the 100% Pt layer. At near-ambient temperature, the adsorption of CO at the Ti sites is dissociative and at the Pt sites, molecular. The orderly substitution of Ti for Pt atoms in the surface changes the Pt–Pt pair site distribution such as to eliminate most of the sites for bridge bonding of the CO molecule. Only a single symmetric TDS peak was observed for CO desorbing from the alloy surface, as opposed to the asymmetric peak shape observed from pure Pt surfaces, which we suggest is a consequence of bridge-site elimination. At low temperature (230 K), a second molecular state of CO was observed which we assigned to a predissociative state on Ti sites with CO lying parallel to the surface. No hydrogen could be observed to desorb from clean annealed Pt_3Ti surfaces dosed with hydrogen at room temperature. Unfortunately, we were not able to distinguish between the possibilities (1) that hydrogen does not adsorb on the surface at room temperature, and (2) that hydrogen adsorbed at room temperature is not desorbed by flashing the surface temperature to ca. 900 K.

1. INTRODUCTION

Pt_3Ti is an intermetallic compound which can be considered representative of a class of compounds (Engel–Brewer type) (*1*), characterized by a highly negative enthalpy of formation, which have been the object of intensive study for their catalytic properties in the reduction of oxygen to water in fuel cells (*2*). The adsorptive properties of an intermetallic compound of this type are of interest because the strength of the intermetallic bond is likely to favor the formation of a well-ordered surface where enrichment phenomena are expected to play a minor role (*3–5*). In such a surface, the chemisorptive properties may be modified either by effects due to the dilution of the active atoms in the bimetallic surface (ensemble effects) or by modifications of the electronic properties of the atoms due to the intermetallic bond (ligand effects). Another important point relative to this type of surface lies in its relation with "SMSI"-type systems (*6, 7*). In these systems the adsorptive properties of the active metal are strongly modified by the interaction with the support. It is possible that an intermetallic bond plays a fundamental role in SMSI and the formation of a compound such as Pt_3Ti was initially suggested as a

[1] Present address: Photometric Inc., Huntington Beach, Calif. 92649.

0021-9517/86 $3.00

possible explanation for SMSI properties (*7*). Although there is an accumulation of evidence implicating TiO_x overlayer formation as the key phenomenon in SMSI (*8–10*), a study of the adsorptive properties of the Pt_3Ti surface may still furnish information on the role of the intermetallic bond in modifying the adsorptive properties of each metal and on the possible relationship of SMSI-type systems to binary Engel–Brewer-type alloys.

In the present study, we used the surface techniques of Auger electron spectroscopy (AES), X-ray photoelectron spectroscopy (XPS), and low-energy electron diffraction (LEED) to characterize the structure and composition of the alloy surface. Thermal desorption spectroscopy (TDS) was the main tool used to investigate the adsorption properties of CO and H_2. The LEED analysis of the structures of $Pt_3Ti(111)$ and $Pt_3Ti(100)$ surfaces is published elsewhere (*11, 12*), and preliminary results for CO and H_2 adsorption on polycrystalline Pt_3Ti appeared in a previous communication (*13*). In the present paper we summarize and discuss all the results obtained in this study both on polycrystalline and on single crystal [100] and [111] oriented Pt_3Ti surfaces. The results show that in all cases the clean surface at equilibrium contains both Ti and Pt atoms in the outermost layer. In general, we observed significant variations in the reactivity of the Pt_3Ti surface with the respect to pure Pt. These variations can be interpreted in part as the result of the geometric effect due to the presence of titanium in the surface and in part as due to electronic effects from the intermetallic bonding.

2. EXPERIMENTAL

Pt_3Ti polycrystalline material was prepared by arc melting the base metals in an argon atmosphere (Ti and Pt nominal purity, 99.99%). X-Ray examination indicated the formation of the fcc $AuCu_3$-type structure (*14*). Single crystal samples were prepared from the polycrystalline material by recrystallization in a zone melting furnace. Samples oriented along the [001] and [111] directions by Laue diffraction methods were spark cut from the single crystal material. One of the crystal faces was mechanically polished, while the other was gold brazed on tantalum foil. Tantalum wires were spotwelded on this foil to support the sample and to anneal it by resistive heating. The sample temperature was measured by means of a chromel–alumel thermocouple spotwelded on the tantalum foil. Two different UHV systems were used for the present study. One was equipped with LEED, a single pass CMA with glancing incidence electron gun for AES and quadrupole mass spectrometer for TDS. This system was also equipped with an electron beam evaporator located in a separate chamber. This evaporator was used to coat the sample surface with a Pt film in order to compare the properties of pure Pt and Pt_3Ti under the same experimental conditions. Films of titanium, deposited by means of a Ta–Ti alloy filament, were used for the same purposes of comparison.

The second vacuum chamber was equipped with a MgK_α X-ray source and a hemispherical analyzer with multichannel counting capability (*15*). TDS spectra could also be recorded by means of a quadrupole mass spectrometer. In this chamber, a pure Pt(111) sample was used to compare the properties of pure Pt with those of $Pt_3Ti(111)$.

Due to the different experimental setup, different annealing rates were used for TDS experiments. In the first vacuum chamber, a rate of 26 deg/s was used for the $Pt_3Ti(111)$ surface and higher rates for the (100) and polycrystalline surfaces. In the second chamber, a rate of 6 deg/s was used for the same experiments. The TDS spectra were qualitatively reproducible from the same crystal in the two chambers. However, the CO TDS peaks from the same sample were consistently shifted toward higher temperature in the experiments performed with the higher heating rates. Simple calculations based on the equations re-

ported in (*16*) show that this difference is due solely to the difference in the heating rate.

3. RESULTS

3.1. Clean Surface Characterization

Most of the initial contamination present on the Pt_3Ti surfaces upon introduction in the vacuum chamber could be removed by room temperature ion bombardment. It was not possible, however, to remove all the oxygen and carbon in this way. Further cleaning could be obtained annealing the sample under UHV conditions at temperatures higher than about 500 K, which resulted in the removal of oxygen apparently by reaction with surface carbon to form CO. Usually, after this treatment, only carbon remained on the surface. A further reduction of the carbon could be obtained by a high temperature treatment involving sequential oxygen dosing and thermal annealing. Oxygen dosing must be carefully controlled, since excessive treatment in oxygen can cause the formation of an overlayer of titanium oxide and deplete the subsurface region of Ti. We succeeded eventually in obtaining an oxygen-free surface with less than 5% monolayer contamination of carbon as determined by XPS and by AES (in the latter case using the calibration reported in (*17*)).

In general, the ion bombarded Pt_3Ti surface showed a much higher Ti/Pt signal ratio than the annealed one. This result can be interpreted in terms of preferential sputtering of Pt atoms. Using the model developed in (*18*) with the data for relative sputtering cross sections reported in (*19*), it can be shown that the bombarded surface composition does not correspond to the equilibrium, but it is enriched in Ti as a result of the sputtering process. From this calculation it appears that the enrichment in platinum of the surface observed upon annealing after sputtering is simply the restoring of the equilibrium composition.

The intensity of the Pt and Ti AES peaks can be used to estimate the surface composition of the clean, annealed alloy. The values reported in the literature for the absolute *dN/dE* intensities of these peaks appear to be unreliable for this purpose, since the actual intensity depends in general on the experimental conditions especially in the case of titanium (*20*). Instead, we used evaporated Ti and Pt films as internal standards to calibrate the intensities of the AES signals. The Ti concentration in the surface was assumed to be proportional to the *dN/dE* intensity of the Ti AES peak at 385 eV. Therefore, the Ti concentration in the Pt_3Ti surface can be measured as the ratio of the intensity of the Ti peak for Pt_3Ti and for a pure Ti film. The composition of the Pt_3Ti surface can also be determined by the same procedure from the intensity of the Pt (238 eV) peak using pure Pt films as reference.

Several measurements were performed depositing Pt and Ti films on the polycrystalline Pt_3Ti surface, obtaining a surface composition of 29 ± 2 at.% in Ti based on the Pt AES peak height and a composition of 28 ± 1 at.% in Ti based on the Ti AES peak height. The compositions of the single crystal surfaces were obtained by comparison of the relative Ti/Pt AES peak height ratio to that for the polycrystalline surface. The resulting calculated compositions were 26 ± 2 at.% Ti for the (111) surface and 30 ± 2 at.% Ti for the (100) surface. All the composition analyses are summarized Table 1. These data indicate a nearly bulklike composition of the clean, annealed Pt_3Ti surfaces. We remark, however, that when the surface was oxidized, the relative

TABLE 1

Composition of the Single Crystal and Polycrstalline Pt_3Ti Surfaces, as Determined by AES

Surface type	Ti(387)/Pt(237) *dN/dE*	% Ti
$Pt_3Ti(111)$	1.7	26 ± 2
$Pt_3Ti(100)$	2.1	30 ± 2
Pt_3Ti (polycrystalline)	1.9	28 ± 2

intensity of the Ti AES peaks was much higher, indicating segregation of oxidized titanium species onto the surface. A detailed study of the oxidation process of these surfaces has been reported elsewhere (*21*). We note also that upon annealing a clean Pt_3Ti surface in the absence of reactive gases, no significant variation of the Ti/Pt *dN/dE* ratio was found for temperatures up to about 900 K. For higher temperatures, an irreversible increase of the relative Ti intensity was found, accompanied by an increase of the carbon AES signal. This result is attributed to the formation of titanium carbide on the surface, possibly arising from the reaction with carbon segregating from the interior of the crystal.

The LEED results relative to the $Pt_3Ti(100)$ and (111) surfaces have been reported (*12*) and will be only briefly summarized here. The Pt_3Ti fcc lattice has cell parameters which are less than 1% different from those of pure Pt (*14*). It is, therefore, possible to interpret the Pt_3Ti diffraction patterns as "superstructures" of the basic Pt pattern. Using the Wood notation, the LEED pattern observed for the $Pt_3Ti(111)$ surface corresponds to a $p(2 \times 2)$-type cell, while the pattern relative to the Pt(100) surface corresponds to a $c(2 \times 2)$ cell. These cells correspond exactly to the cells expected from a structural model which assumes that the surface structure of Pt_3Ti derives from simple truncation of the bulk. In such a model, the outermost plane of $Pt_3Ti(111)$ contains exactly 25% Ti atoms, as all (111)-type planes are identical. The $Pt_3Ti(100)$ plane may be either one of two possible alternating (100) planes: one pure Pt and the other containing 50% Ti atoms. In both cases, a $c(2 \times 2)$ LEED pattern would result. These models for the structures of the (100) and (111) surfaces are shown in Fig. 1.

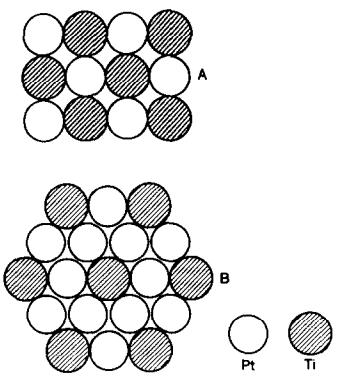

FIG. 1. Models for the structure of the [100] (A) and [111] (B) oriented Pt_3Ti surfaces.

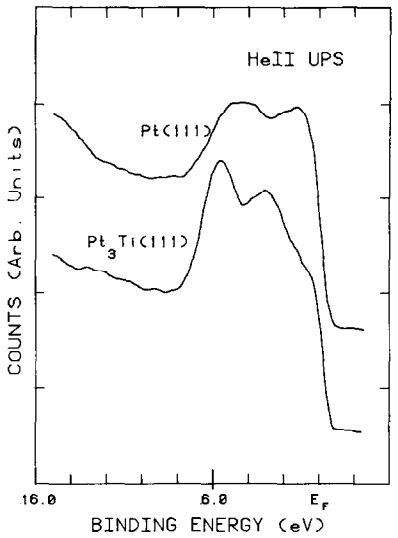

FIG. 2. Comparison of the UPS valence spectra of the Pt(111) and $Pt_3Ti(111)$ surfaces.

3.2. *Adsorptive Properties*

3.2.1. Carbon monoxide. On all three types of Pt_3Ti surface studied, upon exposure to carbon monoxide at room temperature at pressures up to 1×10^{-6} Torr, we obtained evidence of undissociated (i.e., molecular) adsorption from AES and UPS measurements. The carbon KLL AES lineshape results typical of undissociated CO (*22*) and UPS measurements showed the molecular bands of undissociated CO. The He(II) UPS spectra for the clean $Pt_3Ti(111)$ and Pt(111) surfaces are shown in Fig. 2 and the UPS spectra after exposure to CO are shown in Fig. 3. The most

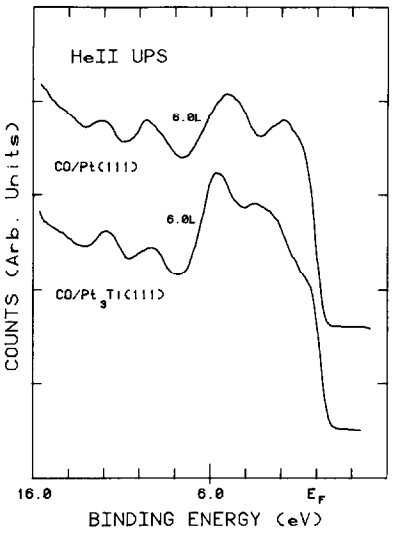

FIG. 3. UPS valence spectra for Pt(111) and $Pt_3Ti(111)$ after saturation with CO at 300 K.

promiment features appearing after CO adsorption are at ca. 9 and 12 eV below E_f, indicative of the $4s$ and 1π–5σ molecular orbital bands of undissociated CO. The main features of the CO molecular bands appear to be the same on both Pt and Pt_3Ti surfaces. However, the XPS data gave a clear indication that a *fraction* of the adsorbed CO dissociates on the surface at room temperature and/or upon flashing the surface to the desorption temperature of the reversibly bound CO. Figure 4 shows the O $1s$–Pt $4p$ region of binding energy for the clean $Pt_3Ti(111)$ surface and for the surface after a 15-L dose of CO and after thermal desorption of the CO. After the thermal flash, an oxygen signal is still detectable. Higher resolution comparison of these features is shown in Fig. 5. The double O $1s$ peak observed here can be compared to the double peak reported by Norton *et al.* (*23*) after CO adsorption on Pt(111). The doublet on Pt_3Ti is much more pronounced, with the low binding energy peak much more intense than on Pt(111). The O $1s$ remnant after flashing is shifted to slightly lower binding energy and corresponds exactly to the O $1s$ peak observed after direct exposure to oxygen of the $Pt_3Ti(111)$ surface. From these data it can be concluded that CO dissociates on part of the Pt_3Ti surface. To determine whether CO dissociates upon adsorption or as an effect of the thermal flashing during TDS experiments, XPS spectra were recorded at incremental temperatures above 228 K. Figure 6 shows the

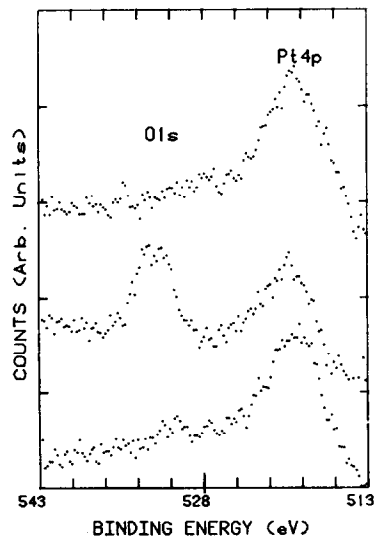

FIG. 4. Oxygen $1s$ XPS spectra on the $Pt_3Ti(111)$ surface: (top) clean surface, (center) after exposure to CO, (bottom) after flash desorption of CO.

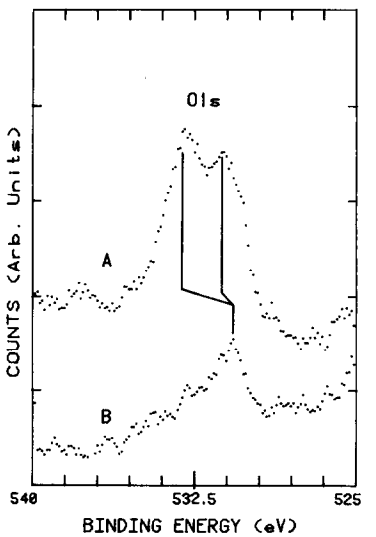

FIG. 5. High-resolution O $1s$ XPS spectra on the Pt_3Ti surface after exposure to CO (A) and after CO thermal desorption (B).

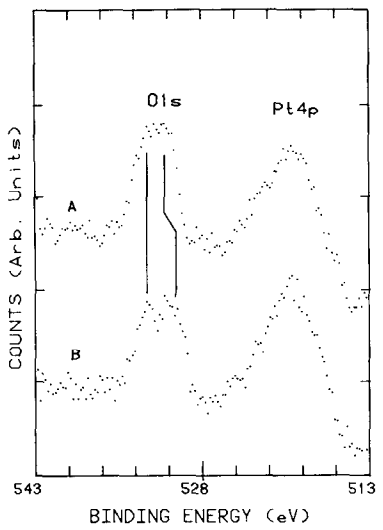

FIG. 6. Comparison of the O 1*s* peak after exposure of the Pt_3Ti surface at (A) 228 K and (B) 313 K.

comparison of the O 1*s* structure at 313 K vs 228 K. The low energy feature of the O 1*s* peak is shifted toward even lower energy at low temperature. This shift can be attributed to a different chemical state of the adsorbed CO at low temperature and possibly to undissociated (molecular) CO adsorbed on Ti atoms with the oxygen end down at Ti sites (*24*).

The relative intensity of the O 1*s* remnant feature on the $Pt_3Ti(111)$ surface after CO thermal desorption was not very reproducible, e.g., variable from ca. 10 to 20% of the total oxygen signal immediately after CO adsorption. Deconvolution of the O 1*s* feature showed that the low binding energy peak is 20 ± 2% of the total peak at 313 K. The poor reproducibility can be attributed to the difficulty in obtaining a perfectly clean Pt_3Ti surface. Therefore, quantitative estimates of the fraction of surface which dissociates CO are not very reliable. However, it is estimated that this fraction is 15–25%, which is consistent with the hypothesis that CO is dissociated only on Ti sites, considering that some of these sites are blocked by carbon contamination at any given time.

The CO thermal desorption spectrum (TDS) for $Pt_3Ti(111)$ is shown in Fig. 7 for variable coverages produced by variable dosing at near-ambient temperature (313 K). The same CO TDS peak shape was observed for $Pt_3Ti(100)$ and for polycrystalline Pt_3Ti. The temperature of the desorption peak maximum shifted to higher temperatures for lower coverages in the same way as it has been observed for pure Pt surfaces. Lowering the adsorption temperature to 228 K increased (+55% higher) the amount of CO desorbing, but did not change the temperature of the desorption peak maximum, as shown in Fig. 8a. However, the XPS results (Fig. 6) indicated that the amount of CO on the surface at saturation at 228 K was only slightly increased from that at 313 K. The dramatic difference in the amount of CO desorbing from the amount adsorbed we attribute to CO dissociation occurring in the temperature interval between 228 and 313 K, as indicated above in the XPS analysis of O 1*s* chemical shifts. A direct comparison of CO TDS between $Pt_3Ti(111)$ and Pt(111) is made in Fig. 8b, where the adsorption temperature was

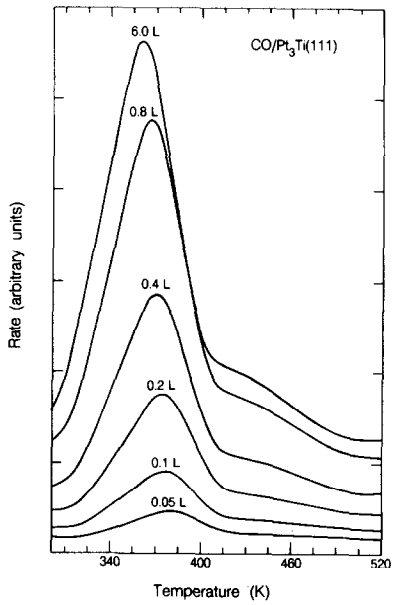

FIG. 7. TDS spectra of CO desorbing from $Pt_3Ti(111)$ as a function of CO dosage (in Langmuirs, L) at 313 K.

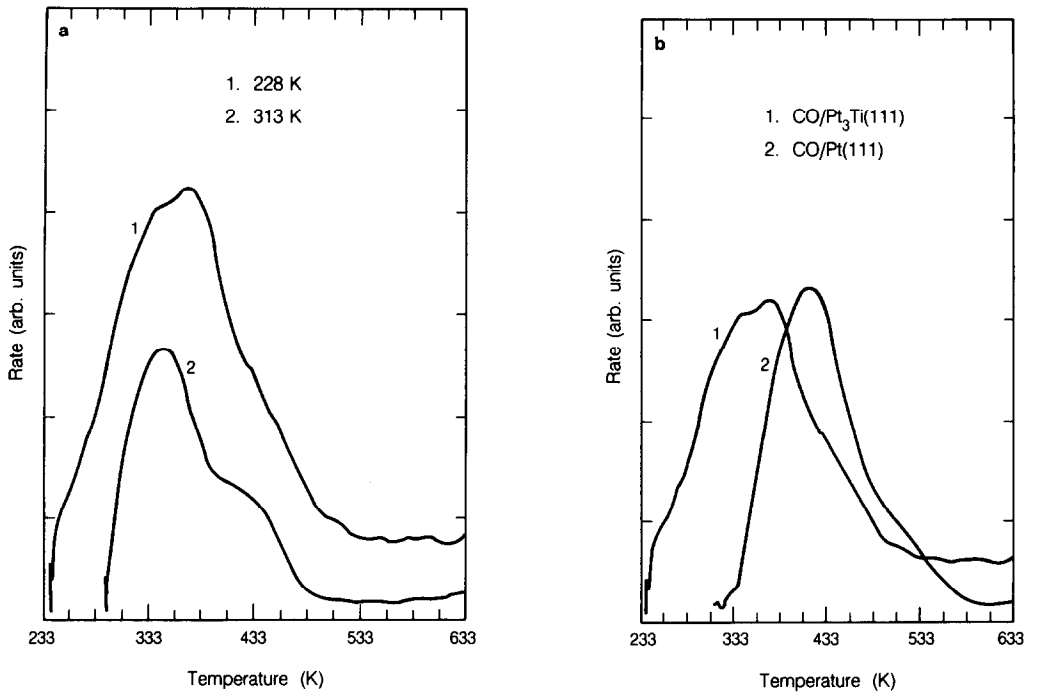

FIG. 8. TDS spectra of CO at saturation (a) on $Pt_3Ti(111)$ and (b) on Pt(111) at 313 K and $Pt_3Ti(111)$ at 228 K.

80 K lower on $Pt_3Ti(111)$ in order to desorb the same quantity of CO from both surfaces. The temperature of the desorption peak maximum at saturation was about 50 K lower on $Pt_3Ti(111)$ than on Pt(111); a similar differential was observed at coverages below saturation, as long as one compared spectra for comparable quantities of CO desorbing.

The area under the CO TDS peak for exposure at the same temperature was always smaller for the Pt_3Ti surface than for the Pt surface; e.g., the ratio of the areas for the alloy and for the pure metal was ca. 0.5 for the (111) oriented surfaces. This value is smaller than expected if we assume that the coverage in terms of CO molecules per platinum atom (only CO on Pt sites desorb intact) is the same in Pt_3Ti as in Pt. This difference appears to be caused by geometric effects due to the dispersion of Ti atoms in the surface, as will be discussed in detail in Section 4.2.

Although the TDS data in Figs. 7 and 8 show temperatures only to 633 K, data were obtained routinely to temperatures of 973 K to look for products of the dissociation reaction, such as the recombination to form CO_2. However, we could not detect anything desorbing from a *clean* Pt_3Ti surface above ca. 500 K. When the Pt_3Ti surfaces were predosed with O_2, then desorption was observed at high temperature. As described in detail elsewhere (*21*), we found that titanium oxide overlayers formed upon exposure of the surface to O_2 (*21*) could block the underlying metal surface to CO adsorption. If the Pt_3Ti surface was only partly oxidized, CO desorption could still be detected. Under these conditions, CO desorption was always accompanied by the formation of CO_2 desorbing at higher temperatures (Fig. 9) and by a partial reduction of the titanium oxide on the surface. No CO_2 desorption could be detected if the surface was not previously oxidized.

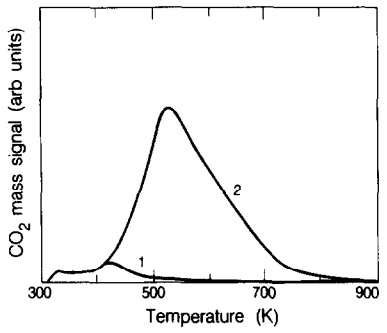

FIG. 9. CO_2 thermal desorption after saturation with CO from (1) clean polycrystalline Pt_3Ti and (2) partially oxidized polycrystalline Pt_3Ti.

Also, CO_2 desorption was not detectable from oxidized Ti in the absence of Pt (i.e., from an oxidized Ti foil).

3.2.2. Hydrogen. Hydrogen adsorption on all three types of surfaces studied was strongly dependent on the previous thermal treatment. On the (111) surface, saturation dosing with H_2 at room temperature after a moderate preannealing (T ca. 500 K) gave rise to the H_2 TDS spectrum shown in Fig. 10a; the corresponding TDS spectrum for the (100) surface after the same treatment is reported in Fig. 10b. The H_2 TDS peak areas were highly sensitive to the annealing temperature and progressively decreased in intensity as the crystals were annealed over ca. 500 K. This progressive disappearance illustrated in Fig. 10b in the case of the $Pt_3Ti(100)$ surface. This result can be attributed only in part to impurities segregating on the surface. The position of the peaks in Fig. 10b is modified as a function of the annealing, a result which is not expected if adsorbing sites are simply sterically blocked. Moreover, AES measurements appear to rule out complete blocking of all Ti sites and show that the amount of surface carbon under these conditions is certainly insufficient to block a significant fraction of the Pt sites. Indeed the presence of free Pt sites was verified by the observation that CO could still be reversibly adsorbed. Although the presence of free Ti sites cannot be considered certain, it appears evident that the lack of H_2 desorption from Pt sites on the Pt_3Ti is not primarily caused by steric blocking.

4. DISCUSSION

4.1. Surface Structure

The first step in understanding the chemical properties of a bimetallic system is to determine the structure and composition of the outermost layer. As is well known, in most cases the surface composition of an alloy differs from that of the bulk. Several theoretical treatments can be applied to exothermic binary alloys in order to predict the surface composition. Van Santen and Sachtler (*4*) have developed a treatment based on the "broken bond" model for the Pt_3Sn compound, which has the same

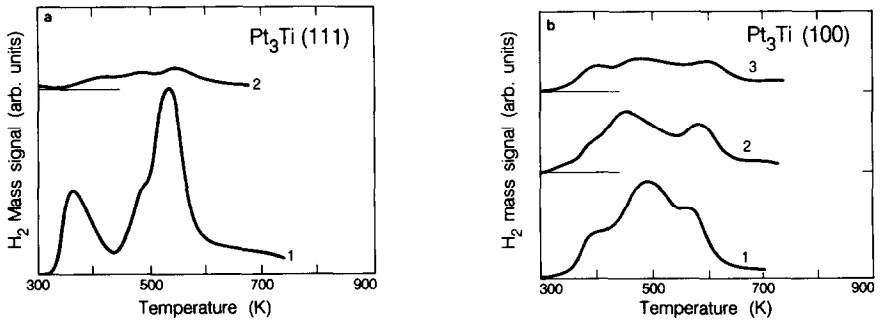

FIG. 10. (a) H_2 thermal desorption spectra from the $Pt_3Ti(111)$ surface: (1) surface preannealed at 573 K; (2) surface preannealed at 1198 K. (b) Effect of successively higher preannealing temperature on the H_2 thermal desorption spectra from $Pt_3Ti(100)$: (1) 623 K, (2) 973 K, (3) 1093 K.

$AuCu_3$-type structure as Pt_3Ti. Pt–Ti alloys of variable stoichiometry have been examined by Spencer (*3*), again using an approach based on the broken bond model. A more sophisticated treatment of surface enrichment in exothermic alloys, valid for the (110) plane of a 1 : 1 alloy, has been developed by Moran-Lopez and Falicov (*5*). From a qualitative viewpoint, all these treatments indicate that, in general, a highly negative enthalpy of formation does not favor surface enrichment at low temperature, and, therefore, the surface composition of Pt_3Ti should be similar to that of the bulk. This conclusion is explicitly stated in (*3*) for the Pt_3Ti stoichiometric compound, although it is also stated that Ti segregation should occur for lower (non-stoichiometric) titanium contents. The latter prediction agrees with the usually valid prediction that the surface will be enriched in the component which has the lower enthalpy of sublimation. Enrichment should also occur by exchange of atoms in the two outermost surface planes. Another prediction of the theory (*4*) is that, below the critical temperature, the surface composition should be weakly dependent on temperature.

The relative tendency of Pt_3Ti to show surface enrichment in comparison to other alloys can be illustrated by the following calculations. It can be shown (*4*, *5*) that in a binary intermetallic compound, the degree of surface enrichment is correlated to a dimensionless parameter, Δ, defined as

$$\Delta = (U_{aa} - U_{bb})/(U_{aa} + U_{bb} - 2U_{ab})$$

where "U_x" are the pair energies relative to the A and B components of the alloy. In general, low values of Δ correspond to little or no surface segregation. From the heats of sublimation of Pt and Ti (*1*) and from the enthalpy of formation of Pt_3Ti (*25*), we can estimate the value of the pair energies and obtain a value of $\Delta(Pt_3Ti) = 0.26$. This value is very small in comparison to that of other isostructural alloys, such as $AuCu_3$ (Δ = 1.37) and Pt_3Sn (Δ = 1.44). The low value for Pt_3Ti is due to two factors: the high value of U_{ab} (27.4 kcal/mol) and the small difference between U_{bb} (18.8 kcal/mol) and U_{aa} (22.4 kcal/mol). The calculated value of Δ can be used for an estimation of the amount of surface segregation on the basis of the results reported in (*5*). These results show that in an exothermic alloy surface enrichment is negligible for Δ values of the order of the one calculated for Pt_3Ti, as long as the temperature is much below the critical temperature (for order–disorder transformation) value. Since the critical temperature for Pt_3Ti can be estimated as higher than 1800 K, it can be concluded that in the range of temperatures used in the present study surface enrichment should play a very minor role in the Pt_3Ti surface in comparison to other alloys, and that most likely no surface enrichment should occur at all.

Experimentally, the AES and LEED results are in good agreement with the above theoretical predictions. First, we observed no dependence of the ratio of the Ti and Pt AES signal on temperature, in agreement with one of the predictions. Second, both the LEED results and the results of the AES measurements (Table 1) show that the surface composition is close to that of the bulk. $Pt_3Ti(111)$, in particular, may have a composition of the outermost layer which is identical to that of the bulk. The $Pt_3Ti(100)$ surface, instead, appears to contain more titanium. This fact is explainable assuming that, of the two possible (100) planes in Pt_3Ti, the one with a 1 : 1 ratio of Pt and Ti atoms forms the outermost layer, while the other (composed of pure Pt) forms the second outermost layer. This hypothesis is in agreement with the results of dynamical calculations of the LEED intensities (*11*). Calculations of the relative intensities of the Ti and Pt AES peaks based on the Gallon formalism (*26*) show that this model is compatible with the Ti(387 eV)/Pt(235 eV) dN/dE ratios observed for the $Pt_3Ti(111)$ and $Pt_3Ti(100)$ surfaces (Table 1).

4.2. *Chemisorption Properties*

In general, the chemisorptive properties of a metal in a binary alloy change only slightly, or not at all, in comparison to the reactivity of the same metal in pure form. This rule is followed by many of the binary alloy surfaces studied so far (*27, 29*). However, our results for the Pt_3Ti surface show that the adsorptive properties of CO and H_2 are considerably changed in comparison to those relative to pure platinum. We performed experiments on Pt and Ti films as well as on a (111) oriented Pt sample to compare the properties of Pt_3Ti with those of the pure metals. In general, the results were in agreement with the available literature data on the adsorptive properties of platinum and titanium.

Considering titanium first, it is known that hydrogen diffuses into the titanium bulk after adsorption and that the CO molecule dissociates, at least in part, on the titanium surface (*30, 31*). Titanium also reacts rapidly with oxygen forming a surface oxide (*32*). All these results could be reproduced in our apparatus with Ti films.

Platinum has a more complex behavior. It is known that CO is molecularly bound to the Pt surface and it has been shown that the CO TDS spectrum depends strongly on the Pt surface morphology. The presence of defects on the surface affects the adsorption parameters (*33*). In general, polycrystalline Pt gives rise to a double CO desorption peak (*33, 34*). Single crystal Pt faces have a different behavior: the (111) face shows a single CO desorption peak, with a maximum for saturation coverage reported in the range 410–420 K by several authors (*33, 35–38*). The same maximum is reported at much higher temperatures by other authors (*39, 40*), presumably as the result of the presence of defects in the surface. We found a value of 413 K for the maximum of this peak (Fig. 8b). The Pt(100) surface has a more complex TDS CO spectrum, showing at least two peaks (*37, 39*) at temperatures similar to those relative to the polycrystalline surface. Considering H_2 adsorption, the literature data (*41–43*), as well as our experiments, agree on the fact that a single H_2 desorption peak is detectable from clean polycrystalline Pt after room temperature exposure. However, the peak area decreases if the Pt surface is "smoothed" by high temperature annealing, indicating that surface defects play a major role in the adsorption of hydrogen on the surface (*33*), a result confirmed by studies of H_2 adsorption on stepped surfaces (*44, 45*).

In comparing the results relative to CO adsorption of the alloy and of pure Pt and Ti, it might be expected that titanium in the alloy surface may behave like titanium metal and dissociation of CO at titanium sites is a possibility. From analyses of both the XPS and TDS data, it is clear that *some* CO dissociates on part of the Pt_3Ti surface, with a proportionality consistent with the hypothesis that the dissociation occurs at titanium sites. This result is in keeping with the known properties of titanium metal and with previously observed reactivity of titanium sites on the Ni_3Ti alloy surface (*46*).

In general, modification of the chemisorptive properties of metals in alloys can be attributed to two different factors: (1) ensemble effects and (2) ligand effects (*27–29*). Ensemble effects are caused by the disappearance (or reduction in number) of specific adsorption sites caused by the dilution of like atoms in the surface. Ligand effects are caused instead by a modification of the electronic properties of one or both metals caused by the intermetallic bond. It is obvious that both effects can play a role in the surface properties of an alloy, and it is often difficult to separate the parts of each. However, the Pt_3Ti single crystal surfaces are formed by an ordered array of Pt and Ti atoms, so that, in this specific case, considerations based on the surface structure should be helpful in establishing the role of "geometric effects," i.e., site modification effects.

If the surface structure of Pt_3Ti corre-

sponds to the model developed in the previous section (that is, bulk truncation), then titanium atoms are dispersed in the surface in such a way as to be in contact only with platinum atoms, independently of the crystallographic orientation of the surface. On the other hand, Pt–Pt bonds are still present. On the (111) oriented Pt_3Ti surface, the Pt sites necessary for the adsorption of CO in both top and bridge orientation are present. However, their relative number is not the same as on Pt(111). For this surface, every Pt atom is bound to only 4 Pt atoms in the surface plane in contrast to the 6 Pt–Pt bonds existing in the Pt(111) surface. This has the effect of eliminating 33% of the Pt–Pt bridge sites on the alloy surface which would otherwise exist if the same number of Pt atoms were arranged as in the Pt(111) surface. On the $Pt_3Ti(100)$ surface, neither the "short" Pt–Pt bridge sites nor the Pt 4-fold sites exist. Pt and Ti atoms are arranged in a checkerboard pattern and only mixed 2-fold (Pt–Ti) and mixed 4-fold sites (2Pt and 2Ti) exist.

These changes in the number of specific sites have important effects on CO adsorption. In the $Pt_3Ti(111)$ case, the reduction in the number of bridge sites (33%) may account for the experimental observation that the area of the CO TDS peak is only 0.5 of the peak area relative to Pt(111), instead of the expected 0.75 if only the geometrical area occupied by Ti atoms is considered. The elimination of the Pt 2-fold and 4-fold sites on the $Pt_3Ti(100)$ surface may cause the suppression of the high temperature CO TDS peaks (*13*) typical of polycrystalline and (100) oriented platinum (*37, 39*) that has been attributed to CO adsorbed on these sites (*42, 47*). According to the calculations of Mehandru *et al.* (*24*), the adsorption of CO on mixed Pt–Ti 4-fold sites is energetically unfavorable in comparison to adsorption on top of the Ti sites, which is a dissociative site. The calculation indicated that the A-top site on Pt atoms in the Pt_3Ti surface is the preferred undissociated state of CO, so that only a single TDS feature would be expected. It appears, therefore, that most aspects of the CO TDS spectra for the alloy surfaces can be explained by purely geometrical "ensemble" effects.

Considerations based on pure ensemble-type effects cannot, however, explain the shift of the CO TDS peak temperature observed on $Pt_3Ti(111)$ in comparison to Pt(111). Assuming that this peak is produced by CO molecules desorbing only from Pt sites, the shift of the maximum of the peak for $Pt_3Ti(111)$ in comparison to Pt(111) (Fig. 8b) amounts to 50 deg and corresponds to a lowering of the activation energy to desorption from platinum sites on the alloy surface. This energy can be estimated as 14% lower on the $Pt_3Ti(111)$ surface, assuming that the desorption process can be described by an Arrhenius-type equation (*16*). The adsorption energy at zero coverage has been estimated as ca. 28 kcal/mol for CO on Pt(111) (*33, 35, 37*) and can, therefore, be estimated to be ca. 24 kcal/mol for $Pt_3Ti(111)$. These values will be considerably smaller for finite coverages since on both the Pt_3Ti and Pt surfaces the peak temperature decreases with coverage; i.e., the intermolecular interaction is repulsive. Dipole–dipole interactions may play a role in the coverage dependence of the bond energy, but since the temperature difference of the maximum in the CO TDS peak was always ca. 50 K whenever an equal amount of CO desorbed from the alloy and pure Pt, it is a reasonable assumption that the CO–CO repulsion due to dipole–dipole effects is approximately the same on both surfaces. Therefore, to account for the reduced adsorption energy of CO on Pt_3Ti, it appears necessary to invoke the existence of ligand effects, that is, of modifications of the Pt electronic properties due to the intermetallic bond.

According to Brewer (*1*), the stability of the Pt–Ti bond (as well as that of the bond of other alloys of Pt with metals of the IVB and VB groups) can be explained in terms of the interaction of electrons of the *d* orbitals from both metals. Specifically, *d* elec-

trons from Ti (d^3s) would combine with empty Pt d orbitals (d^7sp) to form a filled alloy d band. As a consequence, platinum in the alloy would have fewer atomic-like d orbitals available for CO bonding. The possibility of such an electronic effect is entirely consistent with our UPS results that show a modification of the structure of the valence band in Pt_3Ti indicative of rehybridization (Fig. 2) and XPS data that indicate a charge transfer between Pt and Ti (*48*). The molecular orbital calculations of Mehandru *et al.* (*24*) of CO adsorption on the (100) and (111) faces of Pt_3Ti quantifies the modification of the Pt orbitals due to the intermetallic bonding. The calculation predicts a decrease in the binding energy of the CO molecules bound to Pt atoms in the alloy surface if the Ti sites are occupied by a small electropositive adsorbate, such as O produced by dissociation. The calculations also predict that CO should be adsorbed parallel to the surface with the oxygen end on the Ti sites. The calculation indicates weakening of the C–O bond and a low activation barrier to dissociation of the molecule at the Ti sites. All of these predictions were borne out by our experimental observations.

Considering the results for H_2 absorption, the effect of alloying on the adsorptive properties of Pt and Ti atoms in the surface is more complex than in the case of CO. A basic point here is that hydrogen has to be dissociated in order to be adsorbed and must recombine in order to desorb. Both dissociation and recombination phenomena may require more than a single atomic site: an ensemble of 3 Ti atoms has been reported as the site needed to dissociate H_2 on Ti(0001) (*49*) and steps and defects in general are reported necessary for H_2 dissociation on Pt (*33*). Since Pt and Ti are interspersed in an ordered fashion in the Pt_3Ti surfaces, certain types of sites are not available: no Pt–Pt or Ti–Ti nearest-neighbor pairs are present in the (100) surface plane; for the (111) plane no Ti–Ti pairs exist, although Pt–Pt pairs and 3-fold Pt sites exist. Because of this structure, for both (100) and (111) surfaces, a hydrogen atom bonded to titanium can only be desorbed either after recombination with one previously adsorbed on Pt or after moving from a titanium to a platinum site. Another basic point which one must consider for hydrogen adsorption studies by TDS is that in TDS one observes only the hydrogen desorbing from the surface, which does not necessarily represent the amount of hydrogen adsorbed on the surface. Unlike the CO adsorption experiments, AES, XPS, and UPS were not useful (in our experiments) in determining the coverage (or absence) of hydrogen on the Pt_3Ti surfaces. Thus, the fundamental observation we made related to hydrogen adsorption, that little or no hydrogen was observed to desorb from any of the well-annealed stoichiometric Pt_3Ti surfaces, does not enable us to distinguish between the possibilities: (i) that hydrogen is not chemisorbed on the Pt_3Ti surface at room temperature; or (ii) that hydrogen adsorbed on Pt_3Ti surfaces at room temperature is not desorbed by flashing the surface temperature to ca. 900 K. As these two possibilities lead to essentially diametrically opposed conclusions regarding the interaction of hydrogen with the Pt_3Ti surface, a direct determination of hydrogen coverage (or absence) on the surface by another spectroscopy is required before these results can be related to the surface chemistry of Pt_3Ti.

We suggest some similarities in the properties of the Pt_3Ti surface with SMSI-type systems such as Pt supported on reduced TiO_2. According to Tauster *et al.* (*6, 7*), SMSI systems are characterized by the lack of adsorption of CO and H_2 at near-ambient temperature. The Pt_3Ti surface qualified only in part as having SMSI-type adsorptive properties since, although H_2 adsorption appears to be suppressed on annealed surfaces, CO adsorption is still present. The shift toward low temperatures of the CO TDS peak is, however, indicative of a lower adsorption energy, so that the prop-

erties of the Pt_3Ti surface can be seen as intermediate between those of pure Pt and of Pt/reduced TiO_2. When the Pt_3Ti surface is partly oxidized, the formation of CO_2 upon exposure to CO is a reaction which does not occur on Pt nor on titanium oxide. This observation points toward a special synergic effect of surfaces where moieties of oxidized Ti and active metal (Pt) coexist, as suggested by some recent studies of the SMSI effect (*9, 10*).

5. CONCLUSION

The structures of the $Pt_3Ti(111)$ and $Pt_3Ti(100)$ surfaces are formed by simple truncation of the bulk lattice. These surfaces consist of ordered arrays where both Pt and Ti atoms are present with a known distribution of adsorption sites of different types, e.g., Pt–Pt and Pt–Ti pair sites, 3-fold Pt sites, etc. At near-ambient surface temperature, we concluded that CO was adsorbed molecularly on Pt sites while it was dissociated on Ti sites. At sufficiently low temperature, there was evidence of a predissociated molecular state of CO on Ti sites which molecular orbital calculations (*24*) have indicated as an O-end down (i.e., CO molecule lying parallel to surface plane) bonding geometry. CO adsorbed on Pt sites on the alloy surface has a lower binding energy than on pure Pt. This result can be interpreted in terms of both ligand and ensemble effects. Little or no hydrogen was observed to desorb from annealed stoichiometric alloy surfaces. Unfortunately, we could not distinguish experimentally between the possibilities: (i) that hydrogen does not chemisorb on the alloy surface at room temperature; or (ii) that hydrogen adsorbed on the alloy surface does not desorb from the surface upon flashing to 900 K. Some similarities can be found in the behavior of Pt_3Ti and SMSI-type systems such as Pt supported on TiO_2. These similarities suggest that the Pt–Ti bond may play an important role in the chemical properties of a system where both metallic platinum and oxidized titanium interact with gases. However, the fact that the Pt_3Ti surface adsorbs CO at room temperature, in contrast with the properites of SMSI-type systems, indicates that the formation of a binary alloy cannot be taken as the primary factor causing the SMSI effect.

ACKNOWLEDGMENTS

This work supported in part by funds from Consiglio Nazionale delle Ricerche (Italy) and by the Assistant Secretary for Fossil Energy, Office of Fuel Cells, Advanced Concepts Division of the U.S. Department of Energy under Contract DE-AC03-7600098.

REFERENCES

1. Brewer, L., *in* "Phase Stability in Metals and Alloys" (P. Rudman, J. Jaffee, and P. I. Jaffee, Eds.), p. 39. McGraw–Hill, New York, 1967.
2. Ross, P. N., Report EM-1553, Electric Power Research Institute, Palo Alto, Calif., Sept. 1980.
3. Spencer, M. S., *Surf. Sci.* **145,** 145 (1984).
4. Van Santen, R. A., and Sachtler, W. M. H., *J. Catal.* **33,** 202 (1974).
5. Moran-Lopez, J. L., and Falicov, L. M., *Phys. Rev. B* **18,** 2542 (1978).
6. Tauster, S. J., and Fung, S. C., *J. Catal.* **55,** 29 (1978).
7. Tauster, S. J., Fung, S. C., and Garten, R. L., *J. Amer. Chem. Soc.* **100,** 170 (1978).
8. Demmin, R. A., Ko, C. S., and Gorte, R. J., *J. Phys. Chem.* **89,** 1151 (1985).
9. Resasco, D. E., and Haller, G. L., *J. Catal.* **82,** 279 (1984).
10. Sadeghi, H. R., and Henrich, V. E., *J. Catal.* **87,** 279 (1980).
11. Bardi, U., Torrini, M., Zanazzi, E., Rovida, G., Maglietta, M., Ross, P. N., and Van Hove, M. A., *in* "Proceedings, 1st International Conference on Structure of Surfaces, Berkeley, 1984."
12. Bardi, U., and Ross, P. N., *Surf. Sci.* **146,** L555 (1984).
13. Bardi, U., Somorjai, G. A., and Ross, P. N., *J. Catal.* **85,** 272 (1984).
14. Krautwasser, P., Bhan, S., and Schubert, K., *Z. Metallkde.* **59,** H9 (1968).
15. Kevan, S., Ph.D. thesis, University of California, LBL 11017, May 1980.
16. Redhead, P. A., *Vacuum* **12,** 203 (1962).
17. Biberian, J. P., and Somorjai, G. A., *Appl. Surf. Sci.* **2,** 352 (1979).
18. Shimizu, H., Ono, M., and Nakayama, K., *Surf. Sci.* **36,** 817 (1973).
19. Oechsner, H., *Appl. Phys.* **8,** 185 (1975).
20. Davis, G., Natan, M., and Anderson, K. A., *Surf. Sci.* **150,** 321 (1983).
21. Bardi, U., and Ross, P. N., *J. Vac. Sci. Technol. A* **2,** 1467 (1984).

22. Netzer, F. P., and Matthew, J. A. D., *J. Electron Spectrosc. Relat. Phenom.* **16,** 50 (1974).
23. Norton, P. R., Goodale, J. W., and Selkirk, E. B., *Surf. Sci.* **83,** 189 (1979).
24. Mehandru, S. P., Anderson, A. B., and Ross, P. N., *J. Catal.* **100,** 210–218 (1986).
25. Meschter, P. J., and Worrell, W. L., *Met. Trans.* **7A**, 299 (1976).
26. Gallon, T. E., *Surf. Sci.* **17,** 486 (1969).
27. Kelley, M. J., and Ponec, V., *Prog. Surf. Sci.* **11,** 139 (1981).
28. Sachtler, W. M. H., *Le Vide* **164,** 67 (1973).
29. Sachtler, W. M. H., and Van Santen, R. A., *Appl. Surf. Sci.* **3,** 121 (1979).
30. Eastman, D. E., *Solid State Commun.* **10,** 1033 (1972).
31. Fukuda, Y., Lancaster, G. M., Honda, F., and Rabelais, J. W., *J. Chem. Phys.* **68,** 3447 (1978).
32. Bignolas, J. B., Bujor, M., and Bardolle, J., *Surf. Sci.* **24,** L453 (1971).
33. Collins, D. N., and Spicer, W. E., *Surf. Sci.* **69,** 85 (1977).
34. Winterbottom, W. L., *Surf. Sci.* **36,** 195 (1973).
35. Ertl, G., Neumann, M., and Streit, K. M., *Surf. Sci.* **64,** 393 (1977).
36. Crossley, A., and King, D. A., *Surf. Sci.* **95,** 131 (1980).
37. McCabe, R. W., and Schmidt, L. D., *Surf. Sci.* **66,** 101 (1982).
38. Garfunkel, R., and Somorjai, G. A., *J. Phys. Chem.* **86,** 312 (1982).
39. Lambert, R. M., and Comrie, C. M., *Surf. Sci.* **46,** 61 (1974).
40. Shigeishi, P. A., and King, D. A., *Surf. Sci.* **58,** 379 (1976).
41. Nishiyama, Y., and Wise, H., *J. Catal.* **32,** 62 (1974).
42. Barteau, M. A., Ko, E. J., and Madix, R. J., *Surf. Sci.* **102,** 99 (1981).
43. Schwarz, J. A., Polizzotti, R. S., and Burton, J. J., *J. Vac. Sci. Technol.* **1,** 457 (1977).
44. Christmann, K., and Ertl, G., *Surf. Sci.* **60,** 365 (1976).
45. Christmann, K., and Ertl, G., *Surf. Sci.* **54,** 365 (1976).
46. Fischer, T. E., Kelemen, S. R., and Polizzotti, R. S., *J. Catal.* **69,** 345 (1981).
47. Doyen, G., and Ertl, G., *Surf. Sci.* **43,** 197 (1974).
48. Derry, G. N., and Ross, P. N., *Solid State Commun.* **52,** 151 (1984).
49. Cremaschi, P., and Whitten, J. L., *Surf. Sci.* **112,** 265 (1981).